



HAL
open science

Assessment of facial wrinkles as a soft biometrics

Nazre Batool, Sima Taheri, Rama Chellappa

► **To cite this version:**

Nazre Batool, Sima Taheri, Rama Chellappa. Assessment of facial wrinkles as a soft biometrics. Proceedings of 10th IEEE International Conference and Workshops on Automatic Face and Gesture Recognition (FG), 2013, IEEE, Apr 2013, Shanghai, China. pp.1 - 7, 10.1109/FG.2013.6553719 . hal-01096615

HAL Id: hal-01096615

<https://inria.hal.science/hal-01096615>

Submitted on 17 Dec 2014

HAL is a multi-disciplinary open access archive for the deposit and dissemination of scientific research documents, whether they are published or not. The documents may come from teaching and research institutions in France or abroad, or from public or private research centers.

L'archive ouverte pluridisciplinaire **HAL**, est destinée au dépôt et à la diffusion de documents scientifiques de niveau recherche, publiés ou non, émanant des établissements d'enseignement et de recherche français ou étrangers, des laboratoires publics ou privés.

Assessment of Facial Wrinkles as a Soft Biometrics

Nazre Batool, Sima Taheri and Rama Chellappa,
Department of Electrical and Computer Engineering and Center for Automation Research,
UMIACS, University of Maryland, College Park, MD 20742, USA

Abstract—This paper presents results on the assessment of facial wrinkles as a soft biometrics. Recently, several micro features such as moles, scars, freckles, etc. have been used in addition to more common facial features for face recognition. The discriminative power of facial wrinkles has not been evaluated. In this paper we present results of our experiments on assessment of discriminative power of wrinkles in recognizing subjects. We treat a set of facial wrinkles from an image as a curve pattern and find similarity between curve patterns from two subjects. Several metrics based on Hausdorff distance and curve-to-curve correspondences are introduced to quantify the similarity. A simple bipartite graph matching algorithm is introduced to find correspondences between curves from two patterns. We present experiments on data sets using manually extracted and automatically detected wrinkles. The recognition rate for these data sets using only the binary forehead wrinkle curve patterns exceeds 65% at rank 1 and 90% at rank 4.

I. INTRODUCTION

Face recognition has been a popular application of computer vision for a few decades. Face recognition under challenging conditions such as poor resolution, blur, occlusion, illumination/pose variation, expression and aging is being vigorously studied. Recently, a new area of research in face recognition has focused on analysis of facial features other than typical features e.g. eyes, nose, mouth, chin, ears. These new features, called facial micro-features, facial marks or facial soft biometrics, include but are not limited to scars, freckles, moles, facial shape, skin color, hair color, facial hair, tattoos, eye color, shape of nose, beard, mustache and wrinkles [9], [12], [13], [10], [11], [14]. Detection and analysis of these features have become possible due to the availability of high resolution imaging devices and potentially several applications that can benefit from the exploitation of these features. For example, facial freckles, moles and scars have been used in conjunction with a commercial face recognition software for face recognition under occlusion and pose variation [9], [13]. Another interesting application is presented in [11] where recognition between identical twins was done using a proximity analysis of manually annotated facial marks along with other typical facial features. Miller et al., evaluated the discriminative power of local texture of periocular region vs. full facial texture as a soft biometric trait [12]. A combination of traits such as skin, hair, eye color and the presence of glasses, beard and mustache was used by Ouaret et. al [14] to reduce the search time in a face retrieval application. Although, not meant to be an extensive list of recent efforts, the review presented above points to a new trend and potential use of unconventional facial features in many applications.

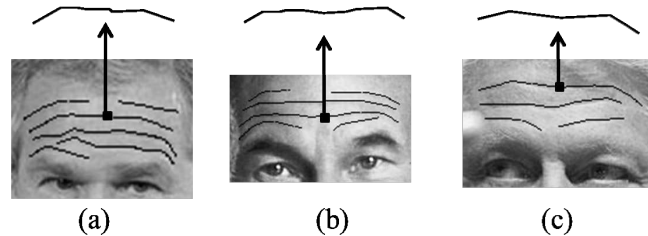


Fig. 1. Different wrinkle patterns with the similar looking curve for three subjects: The curve has been highlighted

The focus of this work is the evaluation of the discriminative power of wrinkles present in human faces and specifically in the forehead areas as a soft biometrics. Whereas the uniqueness of the location of facial marks e.g. moles and scars is very obvious, the uniqueness of wrinkles is not that obvious and has been an unaddressed question so far. The assumption of similarity of wrinkles on the forehead and in areas around the eyes and nose has been widely used in facial aging simulation. For example, few sets of wrinkles were used in [1], [6] to simulate aging faces. An interesting application arises in portrait drawings, sketching, caricatures, etc. of human figures which, most of the time, include sets of wrinkles very specific to that person. This motivates us to ask if a set of wrinkles has sufficient discriminative power to be used as a soft biometrics.

Usually the uniqueness of the facial wrinkles is not very obvious because of two reasons (a) facial wrinkles tend to appear in similar areas of the face i.e. forehead, eye, mouth for most people and (b) the curvature of wrinkle curves is similar in these locations because of factors such as deformations of similar facial muscles for expressions, etc. Hence different subjects tend to have similar wrinkles in similar facial areas. We propose the hypothesis that, although individual wrinkles may be similar in different subjects (e.g. forehead wrinkles, crow feet), a set of wrinkles as a pattern may be unique to an individual. For example, in Figure 1, three subjects are shown to have one very similar wrinkle curve but quite different overall wrinkle patterns. This gives us the motivation to exploit the relative locations of wrinkle curves as a discriminative feature for face recognition.

The problem of wrinkle pattern recognition is challenging due to the large intra class variability caused by several factors. Image acquisition settings play an important role in the appearance of skin texture and, as a result, the visibility of wrinkles. The presence of expressions and/or

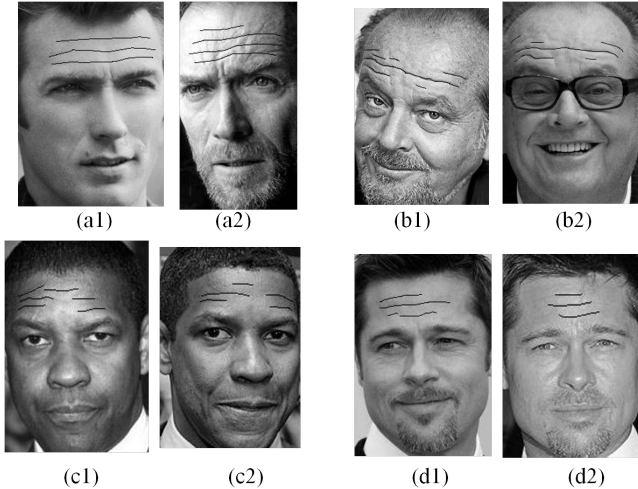


Fig. 2. Images of four subjects with variations in wrinkle patterns due to age, expression and/or image acquisition. Wrinkles have been drawn manually.

pose increases the intra class variability even further by causing spatial displacements of wrinkles as well as changes in their curvatures. Figure 2 shows examples of differences in wrinkle patterns for four subjects. We believe that any attempt at recognizing wrinkle curve patterns has to address the following variations in curve patterns for a single subject.

- 1) Missing Curves
- 2) Discontinuous/Broken Curves
- 3) Deformed Curves

A. Related Work

The wrinkle pattern matching problem can be posed as a matching of two sets of spatially oriented curves. Problems related to curve and shape matching in the presence of distortions and affine transformations have been addressed in the computer vision literature. However, the focus in that research is the recognition of a single open/closed curve and not a set of curves. A more related, and relatively recent, area of research in computer vision community is object recognition/localization using a set of curves or lines [3], [4], [7]. For example, Yu and Leung extended the idea of matching points using Hausdorff distance to matching sets of lines/curves to recognize logos, palm prints and stationary characters. Sets of line segments were also used by Guerra and Pasucci [4] to recognize 3D objects using the Hausdorff distance between the line segment sets. The method was used to extract specific 3D shapes/line patterns from a given image. In this work, we investigate several metrics, mostly based on the Hausdorff distance, to match the wrinkle patterns. Our main contribution is the assessment of the discriminative power of wrinkles in images with uncontrolled acquisition settings. The recognition rate with no facial information other than wrinkle patterns is quite promising. We also present experiments on wrinkles *detected automatically* in some images instead of hand drawn wrinkles. The analysis of person specific wrinkle patterns

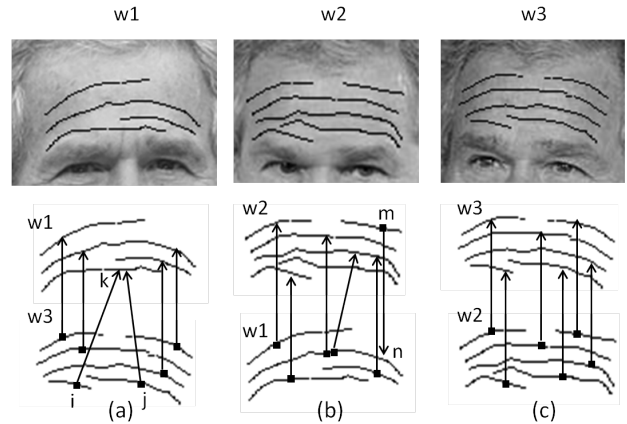


Fig. 3. Three different patterns of wrinkles for the same subject and right correspondences between curves based on spatial proximity

can also be used in applications regarding individual aging patterns in the future.

II. WRINKLE PATTERN MATCHING

In this section, we present the methodology used for wrinkle pattern matching. We take a two step approach to evaluating the similarity between two wrinkle patterns:

- 1) Find one-to-many curve correspondences between two curve patterns.
- 2) Given curve correspondences, calculate the overall distance/similarity between two patterns by combining the distance of each individual correspondence. We call it the *Wrinkle Pattern Distance* (d_{WPD}).

Let the two input binary images representing two wrinkle curve patterns be denoted by $\{\mathbf{I}(x, y); 1 \leq x \leq M_1, 1 \leq y \leq N_1\}$ and $\{\mathbf{J}(x, y); 1 \leq x \leq M_2, 1 \leq y \leq N_2\}$. In binary images the sites corresponding to the wrinkles have value 1 and 0 otherwise. The set of wrinkle curves is represented by \mathbf{V} where each $v_i \in \mathbf{V}$ represents one curve. The coordinates for the image sites belonging to the curve v_i are given by $S_i^v = \{s = (x, y), s \in \mathbb{R}^2\}$. For the rest of the paper, let us denote the Euclidean distance between two points $a \in \mathbb{R}^2$ and $b \in \mathbb{R}^2$ by $d_E(a, b)$. We present the above mentioned two steps in the following sections.

A. Resolving Node/Curve Correspondences

The first task in wrinkle pattern matching is to determine the correspondences between curves in two wrinkle patterns. The correspondences are decided using the three metrics presented in the next section. Figure 3 shows an example of three wrinkle patterns for the same subject. Two of the patterns have 6 curves each whereas one pattern has four curves only. Ideally we want our algorithm to achieve right correspondences as shown in Figure 3 which requires many-to-one matching. In Figure 3(a) the wrinkles ‘i’ and ‘j’ are matched to the wrinkle ‘k’ due to spatial proximity. But in Figure 3(b) the extra wrinkle ‘m’ is matched to ‘n’ which is already matched to two other wrinkles. This eventually increases the mismatch between two patterns. We resolve the

Algorithm 1 Node-to-Node Correspondence Algorithm

 $\mathbf{d}_{sorted} \leftarrow$ sorted array of node distances $\mathbf{d}_v(i, j)$ for all nodes $i \in \mathbf{V}^{(1)}, j \in \mathbf{V}^{(2)}$ in ascending order

 $\mathbf{C} \leftarrow \emptyset$
Step 1:

```

while  $k \leq \text{length}(\mathbf{d}_{sorted})$  do
  if still some nodes in  $(\mathbf{V}^{(1)}, \mathbf{V}^{(2)})$  to be visited then
     $(i, j) \leftarrow$  nodes corresponding to the edge weight
     $\mathbf{d}'(i, j) = \mathbf{d}_{sorted}(k)$ ;
    if  $i$  not visited OR  $j$  not visited then
      include  $(i, j)$  to  $\mathbf{C}$ ;
    end if
  else
    break;
  end if
end while

```

Step 2: Erase extra node associations

```

for  $k = \text{length}(\mathbf{C})$  to 1 do
   $(i, j) \leftarrow \mathbf{C}(k)$ ;
  if both  $i, j$  are included in  $> 1$  correspondences then
     $\mathbf{C}(k) \leftarrow \emptyset$ ;
  end if
end for

```

Fig. 4. Algorithm for finding node-to-node correspondences

curve correspondences as a bipartite graph matching problem by building a fully connected bipartite graph, $G_B^{(1,2)}$. The two sets of curves from two patterns represent two sets of nodes and the calculated distances between curves represent edge weights between nodes. Here we would like to mention that the node correspondence problem is different from the typical bipartite graph matching as follows:

- 1) One popular problem in bipartite graph matching is called ‘minimum weight perfect matching’ where, given equal number of nodes in each partition, every node is matched to exactly one other node while minimizing global edge weights or some other cost function. Our problem does not require the minimization of the overall edge weight functions.
- 2) When the number of nodes in two partitions is different or when the edges are not amenable for one-to-one matching, the problem is posed as a minimum weight constricted (non-perfect) matching. In this case, the graph is fully connected and many to one matching is allowed to accommodate situations where a wrinkle is detected as one curve in one image vs. more than one curves in the other.

This leads us to the following statement for the node correspondence problem.

Given a bipartite graph, not necessarily having the same number of nodes in each partition, find an edge for every node with minimum weight until all nodes have been covered.

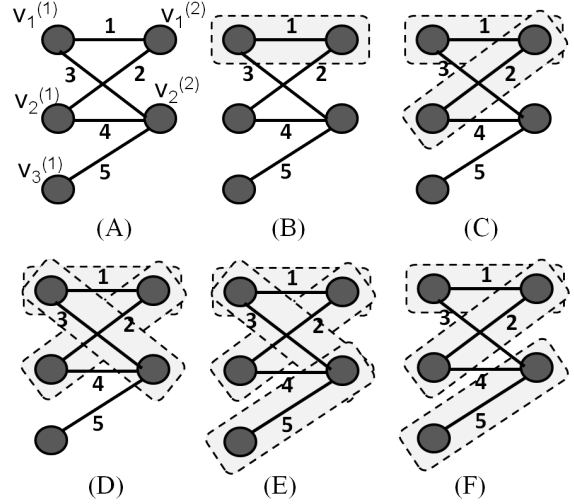


Fig. 5. Step-by-step illustration of our algorithm for finding node correspondences

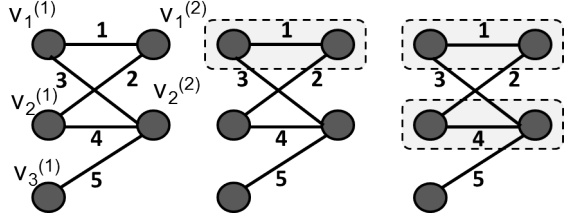


Fig. 6. Step-by-step illustration of a generic bipartite graph matching algorithm with global optimization

Since the number of wrinkles in every pattern is low, we use a greedy approach to solve the problem. Figure 4 presents our algorithm for finding node correspondences. The distance $\mathbf{d}_v(\cdot, \cdot)$ denotes the edge weight between two nodes and can be any of the metrics defined between two curves/nodes in next section. The algorithm has two main steps. At step 1, the edges having at least one node not visited, are included in the increasing order of edge weight. At step 2, the redundant edges are discarded by erasing the edges having both nodes visited more than once in the decreasing order of the edge weight. Figure 5 shows the step-by-step illustration of our algorithm and Figure 6 shows the result of a typical matching algorithm. Our algorithm is different from typical algorithms at steps (c) and (d). At step (c) the edge between $v_2^{(1)}$ and $v_1^{(2)}$ is selected, despite node $v_1^{(2)}$ having been included, over the edge between $v_2^{(1)}$ and $v_2^{(2)}$ due to the lowest edge weight of 2 among the edges connected to $v_2^{(1)}$. At step (f) the redundant edge between $v_1^{(1)}$ and $v_2^{(2)}$ is discarded. Although our algorithm results in a larger global weight of 8 vs. 5 for the typical algorithm, our algorithm results in right spatial correspondences between curves as can be seen in Figure 7.

B. Wrinkles Pattern Similarity Metrics

In this section, we present four different metrics to compare two curve patterns. We start with the modified Hausdorff

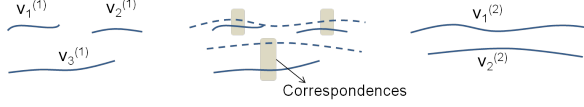


Fig. 7. The curve correspondences achieved using our algorithm

distance [15] which has been widely used as a metric for object recognition based on lines/contours/curves [3], [4], [5], [7]. Then we present three more metrics based on the comparison of pairs of curves in curve correspondences. These metrics compare curve to curve differences in spatial location or shape instead of binary images as a whole as is done in the calculation of modified Hausdorff distance. Following are the detailed descriptions of the four metrics used in our work:

1) *Modified Hausdorff Distance* \mathbf{d}_{MHD} : Given two binary images $\mathbf{I}(x, y)$ and $\mathbf{J}(x, y)$, let $S_{\mathbf{I}} = \{(x, y); \mathbf{I}(x, y) = 1\}$ and $S_{\mathbf{J}} = \{(x, y); \mathbf{J}(x, y) = 1\}$. Then the modified Hausdorff distance $\mathbf{d}_{MHD}(\mathbf{I}, \mathbf{J})$ between two images is given as:

$$\mathbf{d}_{MHD}(\mathbf{I}, \mathbf{J}) = \max(\mathbf{d}_D(S_{\mathbf{I}}, S_{\mathbf{J}}), \mathbf{d}_D(S_{\mathbf{J}}, S_{\mathbf{I}})) \quad (1)$$

where the directed distance $\mathbf{d}_D(A, B)$ is given as follows.

$$\mathbf{d}_D(A, B) = \frac{1}{|A|} \sum_{a \in A} \min_{b \in B} \mathbf{d}_E(a, b). \quad (2)$$

2) *Curve Proximity Distance* \mathbf{d}_{CPD} : We introduce the metric *Curve Proximity Distance* to quantify the spatial proximity of two curves. The main difference between \mathbf{d}_{CPD} and \mathbf{d}_{MHD} is the inclusion of structure of curves. Given curve correspondences, \mathbf{d}_{CPD} is the sum of individual distances for the two curves in a curve correspondence instead of maximum distance for the binary images as a whole in \mathbf{d}_{MHD} . As we will see in the experiments section, the inclusion of curve structure generally improves the recognition rates.

Let l_i and l_j be the lengths of two curves and let $l_{min} = \min(l_i, l_j)$. Then the Curve Proximity Distance, $\mathbf{d}_{CPD}(i, j)$, between the two curves is defined as

$$\mathbf{d}_{CPD}(i, j) = \max(\mathbf{d}_D(S_i^{(1)v}, S_j^{(2)v}), \mathbf{d}_D(S_j^{(1)v}, S_i^{(2)v})). \quad (3)$$

3) *Directed Curve Proximity Distance* \mathbf{d}_{DCPD} : Figure 8 shows the motivation behind introducing this metric by highlighting the difference between the distance \mathbf{d}_D calculated from a shorter curve to a longer curve (Figure 8(a)) and vice versa (Figure 8(b)). This metric allows us to investigate situations where one wrinkle may be represented as one curve in one image vs. more in the other by restricting the metric from being unnecessarily large as can be seen in (Figure 8(c,d)). The $\mathbf{d}_{DCPD}(i, j)$ is defined as follows where $l_{min} = \min(l_i, l_j)$.

$$\begin{aligned} \mathbf{d}_{DCPD}(i, j) &= \mathbb{I}(l_{min} = l_i) \mathbf{d}_D(S_i^{(1)v}, S_j^{(2)v}) \\ &\quad + \mathbb{I}(l_{min} = l_j) \mathbf{d}_D(S_j^{(1)v}, S_i^{(2)v}). \end{aligned} \quad (4)$$

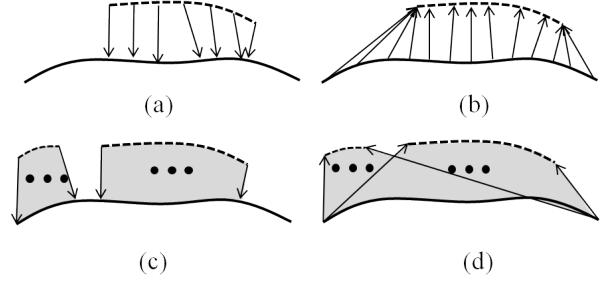


Fig. 8. Difference between shorter to longer vs. longer to shorter distances in \mathbf{d}_{DCPD}



Fig. 9. (Left) Two registered curve patterns (Middle) Calculation of \mathbf{d}_{CSD} (Right) Calculation of \mathbf{d}_{DCPD}

4) *Curve Shape Distance* \mathbf{d}_{CSD} : This metric compares the two curves for their curvature similarity while ignoring their spatial locations in the two curve patterns. The distance is calculated in the same way as calculating the curve proximity distance, however, the curves are aligned with each other. For example, Figure 9 shows the calculation of \mathbf{d}_{CSD} for two curves after aligning them as compared to the calculation of \mathbf{d}_{DCPD} without any alignment. The 2D correlation function is used for alignment. For any two nodes $v_i^{(1)} \in \mathbf{V}^{(1)}$ and $v_j^{(2)} \in \mathbf{V}^{(2)}$, the distance $\mathbf{d}_{CSD}(v_i^{(1)}, v_j^{(2)})$ is calculated as described below.

- 1) Construct two images \mathbf{I}^* and \mathbf{J}^* from input images such that they only have the curves $v_i^{(1)}$ and $v_j^{(2)}$ respectively.

$$\mathbf{I}^*(x, y) = \begin{cases} 1 & \text{if } (x, y) \in S_i^{(1)v} \\ 0 & \text{otherwise} \end{cases} \quad (5)$$

$$\mathbf{J}^*(x, y) = \begin{cases} 1 & \text{if } (x, y) \in S_j^{(2)v} \\ 0 & \text{otherwise} \end{cases} \quad (6)$$

- 2) Use the 2D correlation function to find $s^* = (u^*, v^*)$ as follows

$$\begin{aligned} s^* &= \arg \max_{(u, v)} \sum_{x=1}^{M_1} \sum_{y=1}^{N_1} \mathbf{I}^*(x, y) \mathbf{J}^*(x + u, y + v); \\ &1 \leq u \leq M_1 + M_2, 1 \leq v \leq N_1 + N_2 \end{aligned} \quad (7)$$

- 3) Translate the image \mathbf{J}^* by s^* i.e. $\mathbf{J}_t^*(x, y) = \mathbf{J}^*(x + u^*, y + v^*)$. Thus the curve $v_j^{(2)}$ will also be translated in \mathbf{J}^* . Let us denote the translated curve in \mathbf{J}_t^* as $v_{j_t}^{(2)}$ and the curve in \mathbf{I}^* as $v_{i_t}^{(1)}$.
- 4) Then $\mathbf{d}_{CSD}(i, j)$ is equal to the the curve proximity distance \mathbf{d}_{CPD} between $v_{i_t}^{(1)}$ and $v_{j_t}^{(2)}$.

The overall similarity metric between a probe and a gallery wrinkle pattern, the Wrinkle Pattern Distance, \mathbf{d}_{WPD} , is the

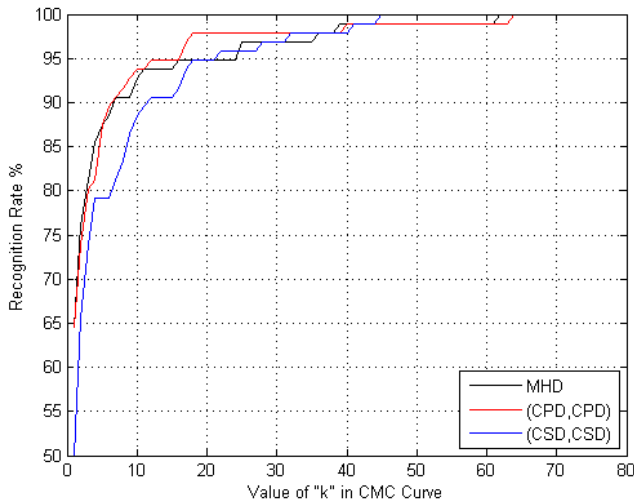


Fig. 10. Comparison of recognition rates for hand-drawn wrinkles.

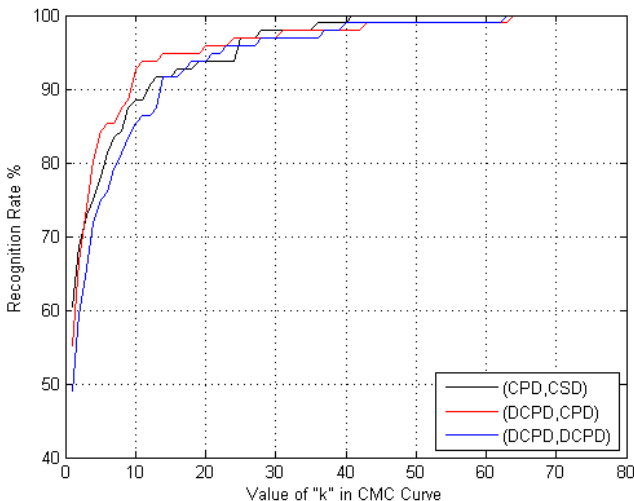


Fig. 11. Comparison of recognition rates for hand-drawn wrinkles

sum of the distance metric for all curve correspondences as follows.

$$\mathbf{d}_{WPD}(\mathbf{V}^{(1)}, \mathbf{V}^{(2)}) = \sum_{c=(i,j) \in \mathbf{C}} \left(\mathbf{d}_v(v_i^{(1)}, v_j^{(2)}) \right). \quad (8)$$

where $\mathbf{d}_v(\cdot, \cdot)$ can be any or a combination of \mathbf{d}_{CSD} , \mathbf{d}_{CPD} and \mathbf{d}_{DCSD} .

III. EXPERIMENTS AND DISCUSSION

To the best of our knowledge, no data set is available in the computer vision community for faces with marked wrinkles. For this work, the data were gathered by selecting images of medium resolution of well-known people from the Internet and consisted of variations of illumination, acquisition setup, pose, expressions and age. The data set comprised of 96 images of 16 subjects with 6 images per subjects. The face images of resolution greater than 200x200 were preferred. The wrinkles were hand drawn by 4 different users. This also

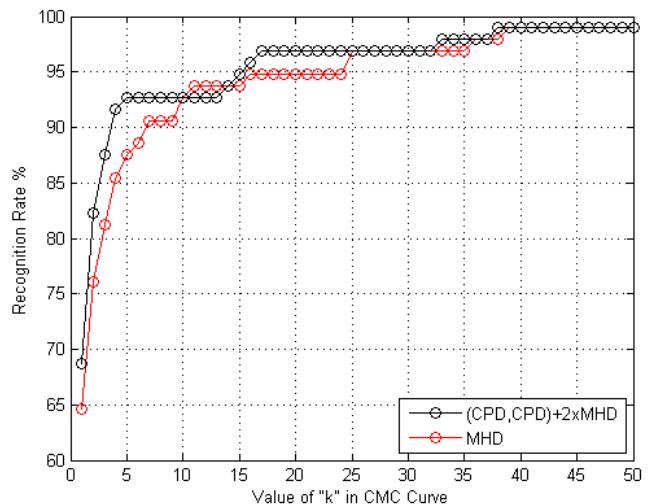


Fig. 12. Comparison of recognition rates for the top two methods

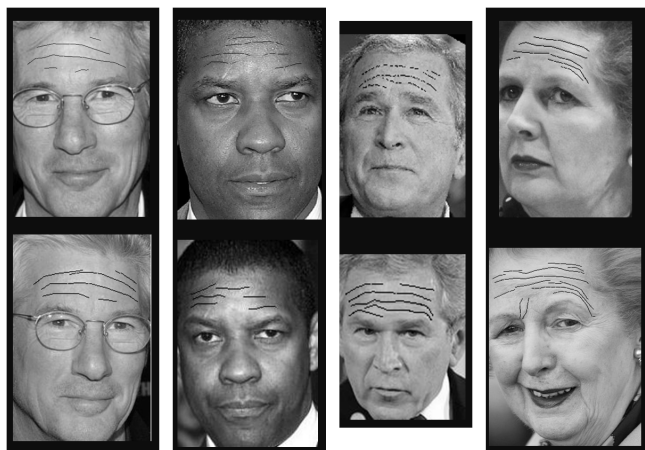


Fig. 13. Four pairs of images where (CPD,CPD) performed better than MHD

included the ‘subjective’ variations in the perception of the wrinkles. The images were registered using five land marks, i.e. two corners of both eyes and the nose tip. As a next step, the wrinkle curves were separated from a binary image by finding connected components followed by morphological processing.

5) *Experiments on Hand-drawn Wrinkles:* Several experiments were conducted on the data set of hand drawn wrinkles with different combinations of the metric used to find correspondences and calculate the distance between curve pairs once the correspondences were established. The cumulative match curves for these experiments are shown in Figures 10, 11 and 12. In the plot legend ‘(a,b)’ means that the metric ‘a’ has been used to find the curve correspondences in algorithm 1 and ‘b’ has been used to calculate \mathbf{d}_{WPD} . Table I shows the percentage recognition rates for the top 5 ranks. We can see that the methods MHD and (CPD,CPD) have comparable results and are better than the rest of the methods. For further investigation the images

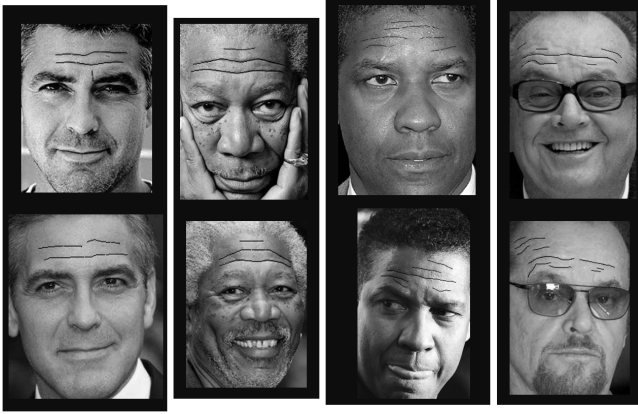


Fig. 14. Four pairs of images where MHD performed better than (CPD,CPD)

where MHD performed better than (CPD,CPD) and vice versa were examined. Figure 13 shows four pairs of wrinkle patterns where (CPD,CPD) was able to recognize correctly in contrast with MHD and Figure 14 shows four pairs of wrinkle patterns where MHD was able to recognize correctly in contrast with (CPD,CPD). As a next step, we combined both MHD and (CPD,CPD) i.e. d_{CPD} was used for finding curve correspondences and $d_{CPD} + 2 * MHD$ was used to calculate d_{WPD} . The combination improved the recognition rate by 5-6% as can be seen in Figure 12 as well as in the last row of Table I.

6) *Experiments on Automatically Detected Wrinkles:* As a next step, we repeated the experiments on automatically detected wrinkles. Recently, the work in [2] reported automatic detection of wrinkles as line segments with average detection rate of 80%. We wanted to investigate if the wrinkle patterns recovered with this detection rate had enough discriminative power. However, the work in [2] detects wrinkles as line segments and the sequences of line sequences are broken at times. We fit curves through line segments to create wrinkle curves. The inclusion of line segments in a curve, however, is not trivial, and requires analysis of the proximity of the line segments. Figure 15 presents our algorithm to include line segments to a curve. The vector of line segments is scanned and a new curve is added whenever an unvisited segment is reached. A sequence of connected line segments is included to a single curve by default. Then a conic region of a certain length and angle is searched around each free end point of a sequence of line segments for any neighboring segments to be included to the same curve. The algorithm outputs the data structure where each node represents a group of line segments to be included in a single curve. Figure 16 shows some examples of the curves fitted to the line segments.

For the automatically detected wrinkles, the experiments were conducted on a data set of 12 images with 3 images per subject. Figures 17, 18 and 19 show plots of the results with different combinations. In the case of detected wrinkles, we observe that the metric combination based on shape, (CSD,CSD), is performing better than MHD and the metric

Algorithm 2 Algorithm for Fitting Curves to Line Segments representing Detected Wrinkles

```

Input: LineSegmentsVector
WrinkleCurveVector  $\leftarrow$  []
while  $k \leq \text{length}(\text{LineSegmentsVector})$  do
   $seg \leftarrow \text{LineSegmentsVector}(k)$ ;
  CurvePoints  $\leftarrow$  [];
  if  $seg$  not visited then  $newSeg \leftarrow seg$ 
  go to Step A;
  repeat
     $newSeg \leftarrow$  The segment connected at RIGHT to  $newSeg$ 
    OR the segment present in RIGHT neighboring conic region
    of  $newSeg$ ;
    go to Step A;
    until border of image reached
  repeat
     $newSeg \leftarrow$  The segment connected at LEFT to  $newSeg$ 
    OR the segment present in LEFT neighboring conic region
    of  $newSeg$ ;
    go to Step A;
    until border of image reached
  end if
Step A:
  Add pixels of  $newSeg$  to curvePoints;
  Mark  $newSeg$  as visited;
return
  Mark  $seg$  as visited;
  Append curvePoints to WrinkleCurveVector;
end while

```

Fig. 15. Algorithm for Fitting Curves to Line Segments representing Detected Wrinkles

combination of (CPD,CPD) both of which had the best performance for hand drawn wrinkles. However the detection rate in this case is lower, 50%, as compared to 64% for hand drawn wrinkles. When we combine both (CSD,CSD) and MHD the recognition rate improves to 90% for top 3 rank positions as can be seen in Figure 19.

IV. CONCLUSION AND FUTURE WORK

In this work we investigated the wrinkles on foreheads as curve patterns for their discriminative power as a soft biometrics. We experimented with different metrics based on the shape and spatial proximity of the curves. The recognition rate achieved by using only the wrinkle patterns

Recognition Rate					
Method	Rank 1	Rank 2	Rank 3	Rank 4	Rank 5
MHD	64%	76%	81%	85%	87%
(CPD,CPD)	64%	74%	80%	81%	88%
(CSD,CSD)	50%	66%	74%	79%	79%
(CPD,CSD)	60%	69%	73%	75%	78%
(DCPD,CPD)	55%	67%	74%	80%	84%
(DCPD,DCPD)	49%	59%	65%	72%	75%
(CPD,CPD)+2xMHD	69%	82%	87%	92%	93%

TABLE I



Fig. 16. (Curves fitted to detected wrinkles as line segments (images were taken from [2])

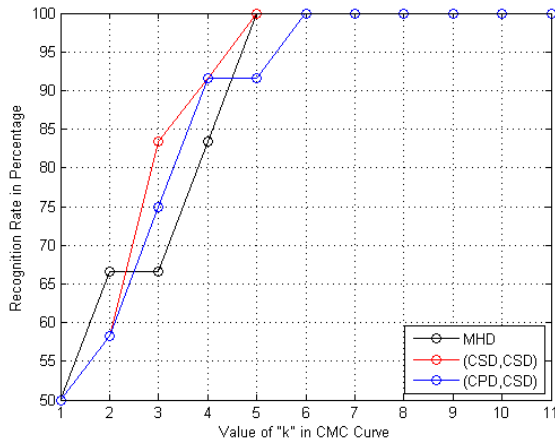


Fig. 17. Comparison of recognition rates for detected wrinkles.

and no other facial features is promising. We also presented the recognition rates on automatically detected wrinkles. This work presents a rudimentary analysis of the wrinkle curves where the information of relative positions/orientations of the curves within the pattern has not been included. In future, the current work can be extended by using more sophisticated pattern matching techniques for the structural information of the curves within a pattern.

ACKNOWLEDGEMENT

The first author would like to acknowledge the support of Fulbright/HEC(Pakistan)/USAID PhD Scholarship. However, this publication has not been approved by the representing agencies/governments of the USA/Pakistan.

REFERENCES

- [1] Narayanan Ramanathan and Rama Chellappa, *Face Verification across Age Progression*, PAMI, Nov. 2006.
- [2] Nazre Batool and Rama Chellappa, *Modeling and Detection of Wrinkles in Aging Human Faces Using Marked Point Processing*, ECCV, 2012.
- [3] Xiaozhou Yu and M. K. H. Leung, *Shape Recognition using Curve Segment Hausdorff Distance*, ICPR 2006.
- [4] Concettina Guerra and Valerio Pascucci, *Line-based object recognition using Hausdorff distance: from range images to molecular secondary structures*, International Journal of Image and Vision Computing, 2005.

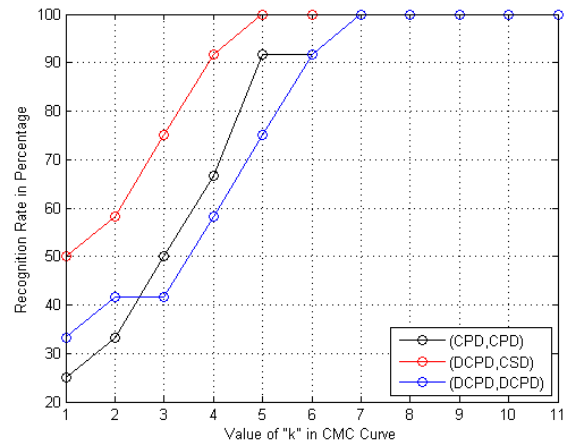


Fig. 18. Comparison of recognition rates for automatically detected wrinkles.

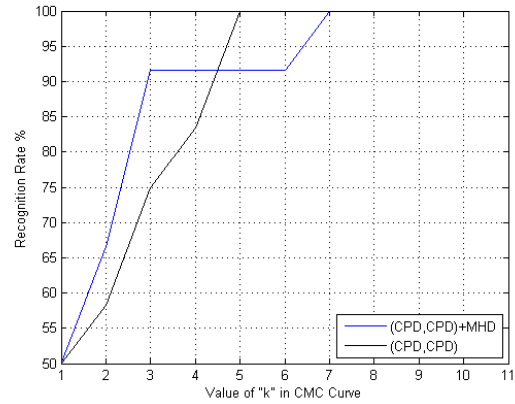


Fig. 19. Comparison of recognition rates for top 2 methods for detected wrinkles.

- [5] William J. Rucklidge, *Efficiently Locating Objects Using the Hausdorff Distance*, IJCV 1997.
- [6] Jinli Suo, Feng Min, Songchun Zhu, Shiguang Shan and Xilin Chen, *A Multi-Resolution Dynamic Model for Face Aging Simulation*, CVPR 2007.
- [7] Xilin Yi, O. I. Camps, *Line-based recognition using a multidimensional Hausdorff distance*, PAMI 1999.
- [8] Laurenz Wiskott, Jean-Marc Fellous, Norbert Krger and Christopher von der Malsburg, *Face Recognition by Elastic Bunch Graph Matching*, PAMI 1997.
- [9] A. K. Jain and Unsang Park, *Facial marks: Soft biometric for face recognition*, ICIP 2009.
- [10] N. D. Srinivas, G. Aggarwal, P. J. Flynn and R. W. V. Bruegge, *Distinguishing identical twins by face recognition*, CVPRW 2011.
- [11] B. Klare, A. A. Paulino, A. K. Jain, *Analysis of facial features in identical twins*, 2011 International Joint Conference on Biometrics 2011.
- [12] P. Miller, J. Lyle, S. Pundlik, and D. Woodard. Performance, *Evaluation of local appearance based periocular recognition*, IEEE BTAS 2010.
- [13] Unsang Park and A. K. Jain, *Face Matching and Retrieval Using Soft Biometrics*, IEEE Trans. on Information Forensics and Security, Sept. 2010.
- [14] Mourad Ouaret, Antitza Dantcheva, Rui Min, Lionel Daniel and Jean-Luc Dugelay, *BIOFACE: a biometric face demonstrator*, ACM Multimedia 2010.
- [15] M. P. Dubuisson and A. K. Jain, *A Modified Hausdorff distance for object matching*, ICPR 1994.